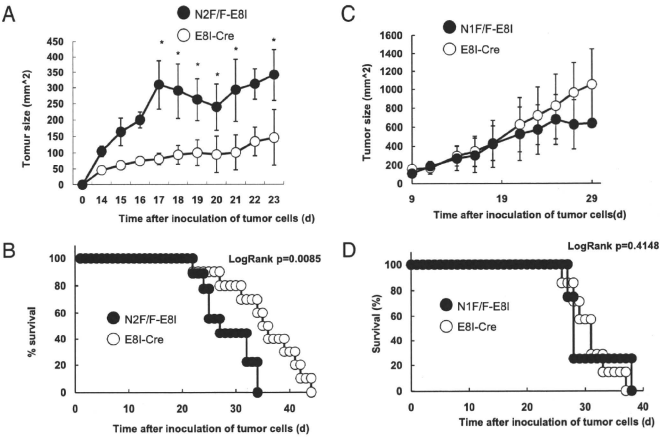

FIGURE 1. Notch2 regulates tumor immune response against EG7. EG7 tumor cells were s.c. inoculated in (*A*, *B*) E8I-Cre (open) and N2F/F-E8I (closed) or (*C*, *D*) E8I-Cre (open) and N1F/F-E8I (closed) mice, and tumor size (*A*, *C*) and mice survival (*B*, *D*) were monitored. Results are shown as mean ± SD. $*p < 0.01$. The experiments are representative of four independent experiments.

endotoxin-free RPMI 1640 medium without FCS and once in endotoxin-free PBS before injection. In some experiments, anti-Notch2 mAb (HMN2-29) (8) or hamster IgG (100 μg/mouse) was injected on days 1, 3, 7, and 10 after tumor inoculation. The anti-Notch2 mAb specifically recognizes Notch2 but not Notch1, Notch3, or Notch4 (Supplemental Fig. 1). Bone marrow-derived DCs (BMDCs) (2×10^6) were injected proximal to the tumor inoculation region 10, 12, and 14 d after tumor inoculation. The BMDCs were infected with delta-like 1 (DL1)- or Jagged2-encoding retrovirus three times as previously reported (8). Then BMDCs were further cultured with irradiated EG7 cells for 2 d before injection, and $CD11c^+$ cells were purified by CD11c magnetic beads (Miltenyi Biotec, Bergisch Gladbach, Germany) before injection into mice. The larger and smaller diameters of the s.c. tumors were measured using calipers at 2-d intervals; these two diameters were multiplied to obtain an estimate of the tumor area. The data are displayed as the mean ± SD of the tumor areas for each group of animals at a given time point.

Vectors and constructs

cDNA for mouse delta-like 1 or Jagged2 was cloned into the retroviral vector pKE004 (11). Retroviruses were generated by transfecting Plat-E cells (12) with vectors using the transfection reagent GeneJuice (Novagen, Darmstadt, Germany). The cDNA for mouse Notch1 or Notch2 was cloned into pcDNA3.1. Each plasmid was transfected into CHO cells by GeneJuice, and a G418-resistant cell line was obtained.

Luciferase assay

CHO cells transfected with Notch1- or Notch2-encoding plasmids were further transfected with a reporter plasmid carrying HES-1 promoter regions (13) and 1.25 ng of the control *Renilla* luciferase reporter plasmid pRL-TK by a Gene Pulser II system (Bio-Rad, Hercules, CA). Anti-Notch2 mAb (10 μg/ml) was added soon after transfection. Twenty-four hours after transfection, luciferase activity was measured by Dual-Luciferase Reporter Assay (Promega, Madison, WI) according to the manufacturer's protocol. Firefly luciferase activity was normalized to *Renilla* luciferase activity using pRL-CMV (Promega). All of the experiments were done in triplicate and repeated at least three times.

Cell purification and cell culture

$CD8^+$ T cells were purified from total spleen or lymph node cells by incubating cells with anti-CD8 mAb (53–6.72), followed by positive selection of $CD8^+$ cells with anti-rat IgG MicroBeads (Miltenyi Biotec). Purified $CD8^+$ T cells (5×10^6) were transferred into C57BL/6 mice that had received EG7 cells 12 d previously. Total spleen cells from OT-I TCR transgenic mice were stimulated with OVA peptide (SIINFEKL) (100 pM) in the presence of anti-Notch2 mAb (HMN2-29) or control hamster IgG (10 μg/ml) for 5 d. The resultant $CD8^+$ cells (1×10^6) were transferred into C57BL/6 mice that had received EG7 cells 12 d previously.

In vitro killing assay

Single-cell suspensions of lymph node cells (2×10^6) were cultured with 1×10^6 irradiated spleen cells for 5 d in the presence of OVA peptide (SIINFEKL) (1 μM) and 5 U/ml human recombinant IL-2. Five days after stimulation, live cells were purified with Lympholyte-M (Cedarlane Laboratories, Hornby, Ontario, Canada) and incubated with target EL4 pulsed with or without OVA peptide and labeled with ^{51}Cr (PerkinElmer, Waltham, MA) at the indicated E:T ratios. After 5 h of incubation, supernatants were harvested, and ^{51}Cr release was measured with a γ scintillation counter (Aloka, Tokyo, Japan). The corrected percentage of lysis was calculated as: corrected % lysis = 100 × (test ^{51}Cr released − spontaneous ^{51}Cr released)/(maximum ^{51}Cr released − spontaneous ^{51}Cr released).

Statistical analysis

All of the data expressed as mean ± SD are representative of at least three different experiments. Comparisons between individual data points were made using Student *t* tests. Differences in survival between experimental groups were analyzed using the Kaplan-Meier approach. The statistical significance of group differences was assessed using the log-rank test. $p < 0.05$ was considered significant.

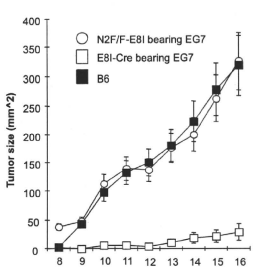

FIGURE 2. Notch2-deficient T cells do not eradicate tumor cells. EG7 tumor cells were s.c. inoculated into E8I or N2F/F-E8I mice. The $CD8^+$ cells from E8I (open square) or N2F/F-E8I mice (open circle) were purified 12 d after inoculation and transferred into C57BL/6 mice that had received EG7 tumor cells 12 d previously. As a control, C57BL/6 mice that did not receive any primed T cells were used (closed square). Results are shown as mean ± SD. The experiments are representative of four independent experiments.

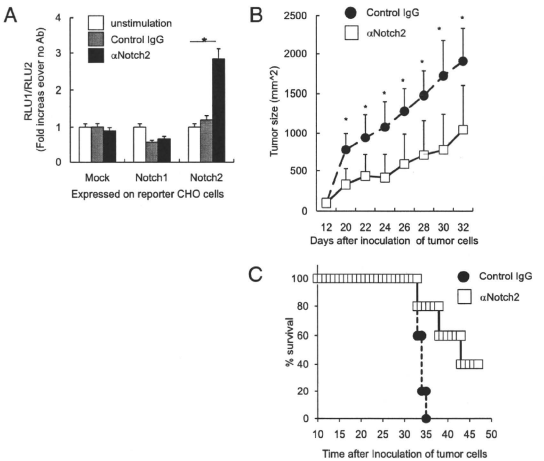

FIGURE 3. Anti-Notch2 agonistic Ab augments antitumor $CD8^+$ T cell responses. *A*, Anti-Notch2 mAb (clone HMN2-29) (black) or control hamster IgG (gray) were incubated with CHO cells transfected with control vector or the cDNA for Notch1 or Notch2. A Notch reporter plasmid was transfected, and luciferase activity was measured and compared with that without an Ab (white). Results are shown as mean ± SD. *B* and *C*, The spleen cells from OT-I TCR transgenic mice were stimulated with OVA peptide (100 pM) in the presence of anti-Notch2 mAb (open square) or control IgG (closed circle) for 5 d in vitro, and purified $CD8^+$ T cells were transferred into C57BL/6 mice that were inoculated s.c. with EG7 tumor cells 12 d before. Then tumor size (*B*) and survival (*C*) of each mouse was monitored. Results are shown as mean ± SD. $*p < 0.01$. The experiments are representative of four independent experiments.

Results

Notch2-deficient mice have lower antitumor activity

We have previously reported that Notch2 has a crucial role in exerting CTL responses (8). To investigate the contribution of Notch2 signaling to $CD8^+$ T cell antitumor immunity, we inoculated EG7 cells (EL4 thymoma cells transfected with the OVA gene) into $Notch2^{flox/flox}$ crossed with E8I-cre transgenic mice (N2F/F-E8I) and control E8I-cre transgenic (E8I) mice. EG7 cells grow gradually in E8I mice, and the growth was much faster in N2F/F-E8I mice (Fig. 1*A*). Accordingly, E8I mice die later than N2F/F-E8I mice after inoculation of EG7 cells (Fig. 1*B*). These data suggest that Notch2 deficiency in $CD8^+$ T cells attenuates EG7 antitumor immune responses.

Because Notch1 is also highly expressed on activated $CD8^+$ T cells (8), we next used $Notch1^{flox/flox}$ crossed with E8I-cre transgenic mice (N1F/F-E8I) inoculated with EG7 cells to determine whether Notch1 deficiency on $CD8^+$ T cells reduces T cell-mediated antitumor immune responses. In contrast to N2F/F-E8I mice, EG7 cells inoculated into N1F/F-E8I mice grow comparable to those in E8I mice (Fig. 1*C*), and N1F/F-E8I mice die with kinetics similar to those seen in E8I mice (Fig. 1*D*). These data indicate that Notch2 on $CD8^+$ T cells contributes to antitumor immunity.

Notch2-deficient mice do not generate antitumor CTLs

We next examined whether tumor Ag-specific killing activity is defective in N2F/F-E8I mice. N2F/F-E8I or E8I $CD8^+$ T cells were harvested from spleen and lymph nodes and enriched from mice 12 d after inoculation of EG7 cells. These cells were then transferred into naive C57BL/6 mice in which EG7 cells had been inoculated 12 d previously. EG7 cells grew poorly in C57BL/6 mice that received T cells from E8I mice, indicating the presence of strong tumor-specific CTLs (Fig. 2). In contrast, EG7 cells grew rapidly in C57BL/6 mice that received T cells from N2F/F-E8I mice, similar to mice in which naive T cells were transferred (Fig. 2). These data indicate that N2F/F-E8I mice are not able to generate enough or high-quality tumor Ag-specific CTLs.

Stimulation of Notch2 by a specific Ab augments antitumor immune responses

We next determined whether overstimulation of Notch2 augments antitumor immune responses. CHO cells were transfected with the genes for mouse *notch1* or *notch2*. These cells were next transfected with Notch reporter plasmids and stimulated by anti-Notch2 mAb. The anti-Notch2 mAb stimulated Notch-mediated

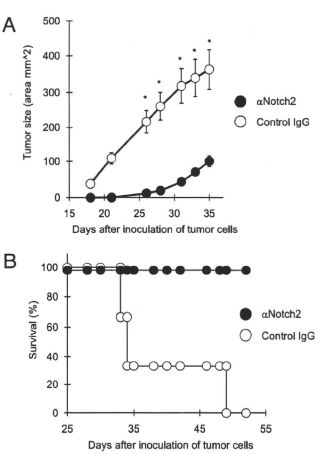

FIGURE 4. Treatment of mice with anti-Notch2 agonistic Ab promotes antitumor immunity in vivo. EG7 tumor cells were s.c. inoculated into C57BL/6 mice that 12 d later received control IgG (open) or anti-Notch2 mAb (closed) 3, 6, 7, and 10 d after tumor inoculation. Tumor size (*A*) and mouse survival (*B*) were monitored every day. Results are shown as mean ± SD. $*p < 0.01$. We used at least five mice in each group, and the experiments are representative of four independent experiments.

signaling only in CHO cells transfected with Notch2 and not Notch1, as evaluated by a HES-1 reporter gene system (Fig. 3*A*). The anti-Notch2 mAb stimulates Notch2 in a concentration-dependent manner, and this stimulatory effect was blocked in the presence of γ secretase inhibitor (Supplemental Fig. 2).

The $CD8^+$ T cells from OT-I TCR transgenic mice were activated with OVA peptide in the presence or absence of anti-Notch2 mAb for 5 d in vitro. Then activated $CD8^+$ T cells were transferred into C57BL/6 mice that had received EG7 cells 12 d previously, and tumor size (Fig. 3*B*) and mouse survival (Fig. 3*C*) were monitored. $CD8^+$ T cells stimulated with anti-Notch2 mAb exhibited greater suppression of tumor growth and enhanced mouse survival compared with those of mice receiving activated control cells (Fig. 3*B*, 3*C*). We did not observe any death at least until day 70 in anti-Notch2 mAb-treated mice that survived at day 50 (data not shown).

Anti-Notch2 mAb promotes the eradication of tumor cells in vivo

We next injected anti-Notch2 mAb or control hamster IgG in C57BL/6 mice that had received EG7 cells 12 d previously. Treatment of tumor-bearing C57BL/6 mice with anti-Notch2 mAb inhibited the growth of EG7 cells compared with that of control IgG (Fig. 4*A*). Similarly, treatment of C57BL/6 mice with anti-Notch2 mAb enhanced mouse survival, and significantly, all mice eventually eradicated the tumor cells (Fig. 4*B*). In addition, we have observed similar antitumor effects of anti-Notch2 mAb when 50 μg Ab in each injection was used (data not shown). These data indicate that stimulation of Notch2 promotes the eradication of tumor cells in vivo.

Delta-like 1-transfected dendritic cells suppress tumor growth

DC-mediated tumor immunotherapy is widely used in clinical settings currently. We have previously reported that DL1 upregulates CTL activity (8). To determine whether DCs overexpressing DL1 (DL1-DCs) are able to suppress tumor growth in vivo, we three times peritumorally injected DL1-DCs or control DCs (cont-DCs) that had been cultured with irradiated EG7 cells in vitro. Tumor cell growth was slower in DL1-DC–injected mice than in cont-DC–injected mice (Fig. 5A). The T cells from draining lymph nodes more highly expressed *hes1*, a Notch target gene, in DL1-DC–inoculated mice than those in cont-DC–inoculated mice (Supplemental Fig. 3). The draining lymph node cells from mice inoculated with EG7 and DL1-DCs or cont-DCs were cultured with irradiated EG7 cells in the presence of IL-2 for 5 d. The cytotoxic activity of T cells against EL4 cells pulsed with OVA peptide was evaluated by ^{51}Cr release assay. No apparent lysis of EL4 cells not pulsed with OVA peptide was exerted by T cells from mice that received cont-DCs or DL1-DCs (Fig. 5*B*). Effector cells from mice that received DL1-DCs exhibited much stronger specific lysis of target EL4 cells pulsed with OVA than effector cells from mice that received cont-DCs (Fig. 5*B*). In addition, we could not detect any cytotoxic activity of T cells from DL1-DC–treated mice if T cells are not cultured in vitro in the presence of

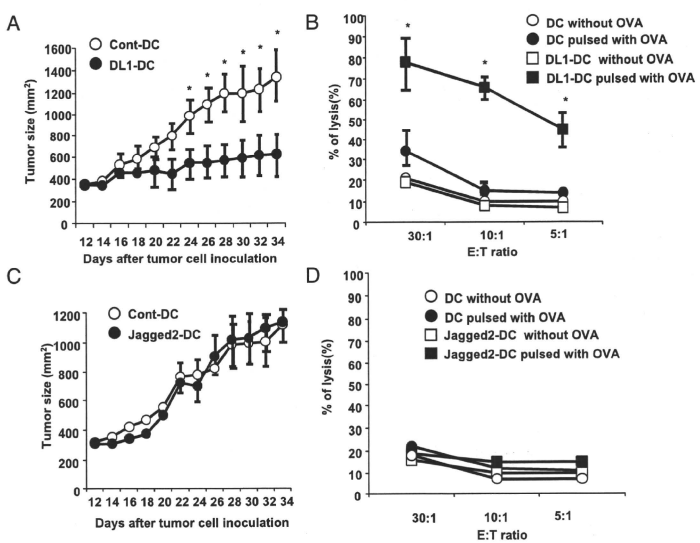

FIGURE 5. Overexpression of delta-like 1 but not Jagged2 on DCs augments antitumor responses by $CD8^+$ T cells. Mouse full-length *dll1* or *Jagged2* was overexpressed in BMDCs (DL1-DCs and Jagged2-DCs) cultured with irradiated EG7 tumor cells for 2 d. (*A*) DL1-DCs (closed) or cont-DCs (open) or (*B*) Jagged2-DCs (closed) or cont-DCs (open) were inoculated into proximal regions of tumors in C57BL/6 mice 10, 12, and 14 d after injecting EG7 cells, and tumor size was monitored. Lymph node cells were recovered 12 d after tumor inoculation and were cultured with irradiated spleen cells in the presence of OVA peptide and recombinant human IL-2 (5 U/ml) for 5 d. Cytolytic activity against EL4 cells pulsed with (closed) or without (open) OVA peptide was evaluated by ^{51}Cr release assay. Killing activity of T cells from mice that received (*C*) DL1-DCs (square), or cont-DCs (circle) or (*D*) Jagged2-DCs (square) or cont-DCs (circle) is shown. Results are shown as mean ± SD. $*p < 0.01$. The experiments are representative of four independent experiments.

OVA peptide (data not shown), probably due to a very low number of Ag-specific T cells. We also tested whether another Notch ligand, Jagged2, has a similar ability to DL1. However, inoculation of DCs transduced with Jagged2 (Jagged2-DCs) did not suppress EG7 growth (Fig. 5*C*), and T cells from Jagged2-DCs did not exhibit cytolytic activity against OVA-pulsed EL4 cells (Fig. 5*D*). The *hes1* expression in T cells from Jagged2-DC–inoculated mice was higher than that from cont-DC–inoculated mice but lower than that from DL1-DC–inoculated mice (Supplemental Fig. 3). Taken together, these data indicate that manipulation of Notch signaling induced by DL1 could be beneficial as a new strategy to augment antitumor CTL activity.

Discussion

Notch signaling controls mature T cell differentiation and activation by directly regulating transcription of effector molecules (7, 8, 14, 15). In particular, our group has recently demonstrated that Notch2 signaling directly controls CTL effector molecules, including granzyme B, by integrating RBP-J and CREB1 (8). In this study, we revealed that Notch2, but not Notch1, signaling in $CD8^+$ T cells is required for efficient induction of antitumor CTLs. Furthermore, treating tumor-bearing mice with anti-Notch2 mAb or DL1-DCs strengthened antitumor CTL responses. These data indicate that Notch2 signaling is required for augmenting antitumor CTL activity and suggest that manipulation of Notch2 signaling might provide a new clinical approach for cancer immunotherapy.

We have recently demonstrated that Notch signaling controls cytotoxic responses in both CTL and NK cells (8, 9). These data suggest that Notch signaling is a crucial signaling pathway required for cytotoxic responses in immune cells. In the studies described in this report, we found that deficiency of Notch2 but not Notch1 decreased the antitumor responses in vivo, although Notch1 is highly expressed on activated $CD8^+$ T cells (8). These data suggest a lower affinity of Notch1 and Notch ligands present in our tumor model relative to those that activate the Notch2 pathway in $CD8^+$ T cells. Notch–Notch ligand interaction is tightly regulated by Notch glycosylation (16), which might be crucial for the distinct Notch receptor utilization controlling CTL responses that we observe. We also found that treatment with anti-Notch2 agonistic Ab in tumor-bearing mice increased antitumor responses. These data strongly suggest that the major target cells for anti-Notch2 mAb in terms of antitumor effects would be $CD8^+$ T cells, although we cannot completely deny the possibility that anti-Notch2 mAb interacts with Notch2 on non-$CD8^+$ T cells, which may indirectly affect Notch2 signaling in $CD8^+$ T cells. Notch2 is widely expressed on many tissues, and thus treatment with anti-Notch2 mAb might have some adverse effects for the host, although we have never seen any macroscopic changes in mice after Ab treatment. Nevertheless, to reduce the possibility of adverse effects of anti-Notch2 mAb, the appropriate route or dose must be considered.

Our previous study showed that DL1 is able to augment CTL responses in vivo (8). We demonstrated in this study that injection of DL1-DCs peritumorally suppresses tumor growth compared with cont-DCs. These data suggest a potential therapeutic strategy to augment antitumor CTLs by injecting DL1-DCs pulsed with tumor-specific Ags. However, we should be cautious with this approach in terms of clinical use because Notch signaling regulates angiogenesis, which nurtures tumor cells (17–19). Those studies revealed that delta-like 4 contributes to angiogenesis. Although the contribution of DL1 to angiogenesis around tumor cells has not been reported, DL1 might also be able to activate Notch receptors that control angiogenesis. Thus, injection of DL1-DCs around the tumor burden may promote angiogenesis for tumor growth, although DL1-DCs would also help to strengthen CTL-mediated killing of tumor cells. The i.v. or s.c. route as a method to transfer DCs has been used in human clinical trials for treating cancer patients. Therefore, it would be important to carefully evaluate whether i.v. or s.c. injection of DL1-DCs affects angiogenesis at the tumor site before applying those methods for clinical use.

In the present work, we have focused on investigating the role of Notch2 signaling in tumor immunity and the effect of anti-Notch2 mAb or DL1-DC treatment on tumor eradication. We show that these treatments enhance survival and decrease the size of the tumor by augmenting CTL activity. The data suggest that stimulation of Notch2 would be a new way to stimulate antitumor immune responses. Combining anti-Notch2 mAb with other therapeutic approaches, such as DC-mediated tumor vaccines, is likely to yield further clinical benefits.

Acknowledgments

We thank Drs. T. Kitamura (Tokyo University, Tokyo, Japan) and I. Taniuchi (RIKEN, Yokohama, Kanagawa, Japan) for providing a cell line and mice, C. Kinouchi for technical assistance, and K. Yamakawa for secretarial assistance.

Disclosures

The authors have no financial conflicts of interest.

References

1. Zou, W., and L. Chen. 2008. Inhibitory B7-family molecules in the tumour microenvironment. *Nat. Rev. Immunol.* 8: 467–477.
2. Caspi, R. R. 2008. Immunotherapy of autoimmunity and cancer: the penalty for success. *Nat. Rev. Immunol.* 8: 970–976.
3. Sutmuller, R. P., L. M. van Duivenvoorde, A. van Elsas, T. N. Schumacher, M. E. Wildenberg, J. P. Allison, R. E. Toes, R. Offringa, and C. J. Melief. 2001. Synergism of cytotoxic T lymphocyte-associated antigen 4 blockade and depletion of $CD25^+$ regulatory T cells in antitumor therapy reveals alternative pathways for suppression of autoreactive cytotoxic T lymphocyte responses. *J. Exp. Med.* 194: 823–832.
4. Curiel, T. J., S. Wei, H. Dong, X. Alvarez, P. Cheng, P. Mottram, R. Krzysiek, K. L. Knutson, B. Daniel, M. C. Zimmermann, et al. 2003. Blockade of B7-H1 improves myeloid dendritic cell-mediated antitumor immunity. *Nat. Med.* 9: 562–567.
5. Radtke, F., A. Wilson, S. J. Mancini, and H. R. MacDonald. 2004. Notch regulation of lymphocyte development and function. *Nat. Immunol.* 5: 247–253.
6. Maillard, I., T. Fang, and W. S. Pear. 2005. Regulation of lymphoid development, differentiation, and function by the Notch pathway. *Annu. Rev. Immunol.* 23: 945–974.
7. Osborne, B. A., and L. M. Minter. 2007. Notch signalling during peripheral T-cell activation and differentiation. *Nat. Rev. Immunol.* 7: 64–75.
8. Maekawa, Y., Y. Minato, C. Ishifune, T. Kurihara, A. Kitamura, H. Kojima, H. Yagita, M. Sakata-Yanagimoto, T. Saito, I. Taniuchi, et al. 2008. Notch2 integrates signaling by the transcription factors RBP-J and CREB1 to promote T cell cytotoxicity. *Nat. Immunol.* 9: 1140–1147.
9. Kijima, M., T. Yamaguchi, C. Ishifune, Y. Maekawa, A. Koyanagi, H. Yagita, S. Chiba, K. Kishihara, M. Shimada, and K. Yasutomo. 2008. Dendritic cell-mediated NK cell activation is controlled by Jagged2–Notch interaction. *Proc. Natl. Acad. Sci. USA* 105: 7010–7015.
10. Saito, T., S. Chiba, M. Ichikawa, A. Kunisato, T. Asai, K. Shimizu, T. Yamaguchi, G. Yamamoto, S. Seo, K. Kumano, et al. 2003. Notch2 is preferentially expressed in mature B cells and indispensable for marginal zone B lineage development. *Immunity* 18: 675–685.
11. Maekawa, Y., S. Tsukumo, S. Chiba, H. Hirai, Y. Hayashi, H. Okada, K. Kishihara, and K. Yasutomo. 2003. Delta1-Notch3 interactions bias the functional differentiation of activated $CD4^+$ T cells. *Immunity* 19: 549–559.
12. Morita, S., T. Kojima, and T. Kitamura. 2000. Plat-E: an efficient and stable system for transient packaging of retroviruses. *Gene Ther.* 7: 1063–1066.
13. Tagami, S., M. Okochi, K. Yanagida, A. Ikuta, A. Fukumori, N. Matsumoto, Y. Ishizuka-Katsura, T. Nakayama, N. Itoh, J. Jiang, et al. 2008. Regulation of Notch signaling by dynamic changes in the precision of S3 cleavage of Notch-1. *Mol. Cell. Biol.* 28: 165–176.
14. Tsukumo, S., and K. Yasutomo. 2004. Notch governing mature T cell differentiation. *J. Immunol.* 173: 7109–7113.
15. Cho, O. H., H. M. Shin, L. Miele, T. E. Golde, A. Fauq, L. M. Minter, and B. A. Osborne. 2009. Notch regulates cytolytic effector function in $CD8^+$ T cells. *J. Immunol.* 182: 3380–3389.

16. Stanley, P., and C. J. Guidos. 2009. Regulation of Notch signaling during T- and B-cell development by *O*-fucose glycans. *Immunol. Rev.* 230: 201–215.
17. Ridgway, J., G. Zhang, Y. Wu, S. Stawicki, W. C. Liang, Y. Chanthery, J. Kowalski, R. J. Watts, C. Callahan, I. Kasman, et al. 2006. Inhibition of Dll4 signalling inhibits tumour growth by deregulating angiogenesis. *Nature* 444: 1083–1087.
18. Noguera-Troise, I., C. Daly, N. J. Papadopoulos, S. Coetzee, P. Boland, N. W. Gale, H. C. Lin, G. D. Yancopoulos, and G. Thurston. 2006. Blockade of Dll4 inhibits tumour growth by promoting non-productive angiogenesis. *Nature* 444: 1032–1037.
19. Siekmann, A. F., and N. D. Lawson. 2007. Notch signalling limits angiogenic cell behaviour in developing zebrafish arteries. *Nature* 445: 781–784.

blood

2010 115: 2872-2881
Prepublished online Oct 27, 2009;
doi:10.1182/blood-2009-05-222836

Hes1 immortalizes committed progenitors and plays a role in blast crisis transition in chronic myelogenous leukemia

Fumio Nakahara, Mamiko Sakata-Yanagimoto, Yukiko Komeno, Naoko Kato, Tomoyuki Uchida, Kyoko Haraguchi, Keiki Kumano, Yuka Harada, Hironori Harada, Jiro Kitaura, Seishi Ogawa, Mineo Kurokawa, Toshio Kitamura and Shigeru Chiba

Blood (print ISSN 0006-4971, online ISSN 1528-0020), is published weekly by the American Society of Hematology, 2021 L St, NW, Suite 900, Washington DC 20036.

Hes1 immortalizes committed progenitors and plays a role in blast crisis transition in chronic myelogenous leukemia

Fumio Nakahara,[1-4] Mamiko Sakata-Yanagimoto,[1,2,5] Yukiko Komeno,[3,4] Naoko Kato,[3,4] Tomoyuki Uchida,[3,4] Kyoko Haraguchi,[1,6] Keiki Kumano,[1,2] Yuka Harada,[7] Hironori Harada,[8] Jiro Kitaura,[3,4] Seishi Ogawa,[9] Mineo Kurokawa,[1,2] Toshio Kitamura,[3,4] and Shigeru Chiba[1,5]

[1]Department of Cell Therapy and Transplantation Medicine and [2]Department of Hematology Oncology, University of Tokyo, Tokyo; [3]Division of Cellular Therapy, Advanced Clinical Research Center, University of Tokyo, Tokyo; [4]Division of Stem Cell Signaling, Center for Stem Cell Therapy, Institute of Medical Science, University of Tokyo, Tokyo; [5]Department of Clinical and Experimental Hematology, Graduate School of Comprehensive Human Sciences, University of Tsukuba, Ibaraki; [6]Division of Transfusion and Cell Therapy, Tokyo Metropolitan Cancer and Infectious Disease Center Komagome Hospital, Tokyo; [7]International Radiation Information Center, Hiroshima University, Hiroshima; [8]Department of Hematology and Oncology, Research Institute for Radiation Biology and Medicine, Hiroshima University, Hiroshima; and [9]Cancer Genomics Project, Graduate School of Medicine, University of Tokyo, Tokyo, Japan

Hairy enhancer of split 1 (Hes1) is a basic helix-loop-helix transcriptional repressor that affects differentiation and often helps maintain cells in an immature state in various tissues. Here we show that retroviral expression of Hes1 immortalizes common myeloid progenitors (CMPs) and granulocyte-macrophage progenitors (GMPs) in the presence of interleukin-3, conferring permanent replating capability on these cells. Whereas these cells did not develop myeloproliferative neoplasms when intravenously administered to irradiated mice, the combination of Hes1 and BCR-ABL in CMPs and GMPs caused acute leukemia resembling blast crisis of chronic myelogenous leukemia (CML), resulting in rapid death of the recipient mice. On the other hand, BCR-ABL alone caused CML-like disease when expressed in c-Kit-positive, Sca-1-positive, and lineage-negative hematopoietic stem cells (KSLs), but not committed progenitors CMPs or GMPs, as previously reported. Leukemic cells derived from Hes1 and BCR-ABL-expressing CMPs and GMPs were more immature than those derived from BCR-ABL-expressing KSLs. Intriguingly, Hes1 was highly expressed in 8 of 20 patients with CML in blast crisis, but not in the chronic phase, and dominant negative Hes1 retarded the growth of some CML cell lines expressing Hes1. These results suggest that Hes1 is a key molecule in blast crisis transition in CML. (*Blood.* 2010;115(14):2872-2881)

Introduction

The balance between activator and repressor basic helix-loop-helix transcription factors is crucial for the proper timing of cellular differentiation and normal morphogenesis of various tissues.[1] During embryogenesis, the basic helix-loop-helix protein hairy enhancer of split 1 (Hes1), functioning downstream of the Notch receptor,[2,3] blocks differentiation of neural stem cells by antagonizing Mash1[4] and affects the cell-fate decision of pancreatobiliary epithelial progenitors.[5] In the adult hematopoietic system, Hes1 blocks granulocyte colony-stimulating factor-induced granulocytic differentiation of the 32D cell line,[6] preserving the long-term reconstituting ability of hematopoietic stem cells (HSCs) in vitro as well as in vivo.[7] Hes1 also plays a significant role in the development of perinatal T cells,[8,9] and knocking out Hes1 leads to lack of thymus.[9]

Recently, activating mutations of the *Notch1* and *Notch2* genes have been identified in more than 50% of human T-cell acute lymphoblastic leukemias[10] and in a subset of non-Hodgkin lymphomas,[11] respectively, implicating Notch signal deregulation based on a genetic abnormality in human cancers. The effect of Notch signal aberration, however, has been largely confined to lymphoid lineages in the hematopoietic compartment. Indeed, enhanced Notch signaling provides the bone-marrow-to-thymus transition stage of early progenitors, with strong selective pressure toward thymic T-cell precursors at the expense of B-cell and myeloid precursors.[12-14] We recently found that up-regulation of Hes1 represents only a part of Notch signaling during the decision between mast cell and granulocyte lineage differentiation. Notch signaling does promote mast-cell development at the expense of granulocyte differentiation through up-regulation of both Hes1 and GATA-3 in common myeloid progenitors (CMPs) and granulocyte-macrophage progenitors (GMPs). However, up-regulation of Hes1 alone causes expansion of cells with myeloid progenitor phenotypes, rather than mast cell development, mediated through down-regulation of a transcription factor, C-enhancer binding protein α (C/EBP-α).[15]

A growing volume of evidence shows that down-regulation of C/EBP-α represents major events in human acute myelogenous leukemia (AML), through either genetic or epigenetic abnormalities. Therefore, it is postulated that Hes1 up-regulation may be involved in a subset of myeloid leukemias.

Chronic myelogenous leukemia (CML) is a myeloproliferative neoplasm that originates in an abnormal pluripotent bone marrow stem cell and is consistently associated with the *BCR-ABL* fusion gene. The disease is biphasic or triphasic; an initial indolent chronic phase is followed by one or both of the aggressive stages, the accelerated phase and blast crisis, resulting in expansion of immature leukemic cells. The mainstay of chronic phase to blast

Submitted May 19, 2009; accepted September 27, 2009. Prepublished online as *Blood* First Edition paper, October 27, 2009; DOI 10.1182/blood-2009-05-222836.

The online version of this article contains a data supplement.

The publication costs of this article were defrayed in part by page charge payment. Therefore, and solely to indicate this fact, this article is hereby marked "advertisement" in accordance with 18 USC section 1734.

crisis transition is the differentiation block by additional genetic events in progenitor stages of CML cells[16] that could otherwise differentiate during the chronic phase. Thus, the transformation of BCR-ABL-induced myeloproliferative neoplasm to full-blown blast crisis has been drawing tremendous attention from investigators.

Here we show that retroviral expression of Hes1 immortalizes CMPs and GMPs in vitro. Hes1 introduction together with BCR-ABL into CMPs and GMPs, the postulated origin of blast crisis transition in CML, induced CML blast crisis-like disease when intravenously administered to sublethally irradiated mice. Considering as well the study of Hes1 expression in CML patients, we propose that Hes1 is a unique experimental tool for studying the mechanisms of chronic phase to blast crisis transformation in CML.

Methods

Mice

C57BL/6 (Ly5.1) donor mice were purchased from Sankyo Labo Service Corporation. C57BL/6 (Ly5.2) recipient mice were purchased from SLC. Mice were kept at the Animal Center for Biomedical Research, University of Tokyo, according to institutional guidelines.

Bone marrow progenitor sort

Bone marrow cells were isolated from the femurs and tibias of C57BL/6 (Ly5.1) donor mice (8-10 weeks of age) and were incubated with biotinylated antibodies for lineage markers, including anti-CD3, anti-CD4, anti-CD8, anti-B220, anti-Ter119, and anti–Gr-1 antibodies (BD Biosciences PharMingen) followed by incubation with streptavidin Micro Beads (Miltenyi Biotec). The lineage marker-negative (Lin^-) fraction was separated with an autoMACS separator or LS Columns (Miltenyi Biotec) and incubated with anti-CD34–fluorescein isothiocyanate, anti-CD16/32 (FcγRIII/II receptor)–phycoerythrin (PE), anti–c-Kit–allophycocyanin, streptavidin peridinin chlorophyll protein (BD Biosciences PharMingen), and anti–Sca-1–PE/Cy7 (eBioscience). $Lin^-c\text{-}Kit^-Sca\text{-}1^+$, $Lin^-c\text{-}Kit^+Sca\text{-}1^-FcγR^{lo}CD34^+$, and $Lin^-c\text{-}Kit^+Sca\text{-}1^-FcγR^{hi}CD34^+$ cells (KSLs, CMPs, and GMPs, respectively)[17] were sorted with a FACSAria cell sorter (BD Biosciences).

Transfection and retrovirus production for murine cells

Rat Hes1 cDNA, a gift from R. Kageyama (Kyoto University, Kyoto, Japan), was subcloned into a retrovirus vector, GCDNsam/internal ribosome entry site (IRES)–nerve growth factor receptor (NGFR), a gift from H. Nakauchi (University of Tokyo) and M. Onodera (National Center for Child Health and Development, Tokyo, Japan). BCR-ABL (p210) cDNA[18] was subcloned into a retrovirus vector, GCDNsam/IRES-GFP.[19] Mouse C/EBP-α cDNA, a gift from K. Akashi (Kyushu University, Fukuoka, Japan) and S. Mizuno (Dana-Farber Cancer Institute, Boston, MA), was subcloned into a retrovirus vector, pMYs-IRES-GFP.[19] Plat-E[20] packaging cells maintained in Dulbecco modified Eagle medium supplemented with 10% fetal calf serum were transfected with retroviral constructs using FuGENE 6 transfection reagent (Roche Diagnostics) according to the manufacturer's instructions. The medium was changed a day after transfection, and retroviruses were harvested 48 hours after transfection, as previously described.[19,20]

Transfection and retrovirus production for human cell lines

We generated a dominant-negative Hes1 (dnHes1) lacking a C-terminal WRPW (Trp-Arg-Pro-Trp) domain as described.[21] The fragment of dnHes1 was subcloned into pMYs-IRES-GFP.[19] Retrovirus packaging was done as described. Briefly, retroviruses were generated by transient transfection of Plat-A[20] packaging cells with FuGENE 6 (Roche Diagnostics).

Infection to progenitors

The retrovirus medium was placed in 24-well nontissue culture dishes for 4 hours at 37°C, precoated with 40 μg/mL of RetroNectin (Takara Bio) overnight at 4°C. After washing the wells with phosphate-buffered saline, sorted KSLs, CMPs, or GMPs were plated for infection for 48 to 60 hours with the coated retroviruses harboring GCDNsam/IRES-GFP-BCR-ABL (p210) or GCDNsam/IRES-NGFR-Hes1 or an empty vector as a control. Infection was done in StemSpan SFEM medium (StemCell Technologies) containing 100 ng/mL mouse stem cell factor (SCF), 100 ng/mL mouse thrombopoietin (TPO), and 100 ng/mL human FLT3 ligand (FL) for KSLs, or in Iscove modified Dulbecco medium (Sigma-Aldrich) containing 20% fetal calf serum, 50 ng/mL mouse SCF, 20 ng/mL mouse TPO, and 20 ng/mL mouse interleukin-3 (IL-3), 20 ng/mL human IL-6 (R&D Systems) for CMPs or GMPs.

Colony-forming assay

Retrovirus-infected cells were sorted at 48 to 60 hours from the initiation of infection with a FACSAria cell sorter (BD Biosciences) and used for colony-forming assay using Methocult 3231 (StemCell Technologies), supplemented with 50 ng/mL mouse SCF, 20 ng/mL mouse TPO, and 20 ng/mL mouse IL-3, 20 ng/mL human IL-6. A total of 1000 cells were cultured in each 2.5-cm dish in duplicate. The colony-forming cells were harvested and replated every 7 to 9 days and scored for colony formation. We defined a colony as "a group of cells, grown from a single parent cell, which is composed of more than 40 live cells."

Mouse bone marrow transplantation

Bone marrow cells prepared from C57BL/6-Ly5.1 mice were infected with retrovirus containing Hes1 or BCR-ABL, and 0.1 to 2.6×10^5 of Hes1/NGFR-sorted or BCR-ABL/GFP-sorted cells were injected through tail veins into C57BL/6-Ly5.2-recipient mice (8-12 weeks of age) after sublethal (5.25 Gy) or lethal (9.5 Gy) total body γ-irradiation (^{135}Cs). For the lethally irradiated mice, 2×10^5 of C57BL/6-Ly5.2 mice-derived bone marrow cells were simultaneously injected for radioprotection. Probabilities of overall survival of the mice that received transplantations were estimated using the Kaplan-Meier method. Statistical differences were determined by the Wilcoxon test. All animal studies were approved by the Animal Care Committee of the Institute of Medical Science, University of Tokyo.

Analysis of mice receiving transplantation

After transplantation, mice were monitored for signs of disease, such as cachexia, hyperpnea, or loss of gloss in fur. Autopsies were performed on moribund recipient mice. Peripheral blood count was analyzed by KX-21 Auto Analyzer (Sysmex). Morphology of the peripheral blood was evaluated by staining of air-dried smears with Hemacolor (Merck). Tissues including bone marrow, spleen, and liver were fixed in 10% buffered formalin, embedded in paraffin, sectioned, and stained with hematoxylin and eosin. Cytospin preparations of bone marrow and spleen cells were also stained with Hemacolor. Percentage of blasts, myelocytes, neutrophils, monocytes, lymphocytes, and erythroblasts was estimated by examination of at least 200 cells. To assess whether the leukemic cells were transplantable to secondary recipients, 0.1 to 5×10^6 total bone marrow cells were injected into the tail veins of sublethally irradiated mice. Two recipient mice were used for each serial transplantation.

Flow cytometric analysis

Red blood cells were lysed using Red Blood Cell Lysing Buffer (Sigma-Aldrich) in peripheral blood or single-cell suspensions of bone marrow and spleen. After washing with phosphate-buffered saline, Fc receptor was blocked by incubating cells with 2.4G2 antibody (eBioscience) for 15 minutes at 4°C and then staining them with the following PE-conjugated monoclonal antibodies for 20 minutes at 4°C: Ly-5.1, Gr-1, CD11b, B220, CD19, CD3, CD4, CD8, c-Kit, Sca-1, CD34, and Ter119. Flow-cytometric analysis of the stained cells was performed with FACSCalibur

(BD Biosciences) equipped with CellQuest software (BD Biosciences) and FlowJo software (TreeStar).

Patients

CML patients were diagnosed at Hiroshima University Hospital and its affiliated hospitals. Diagnosis was based on morphologic, immunophenotypic, and, in some cases, real-time reverse transcription-polymerase chain reaction (RT-PCR) studies according to the French-American-British classification or World Health Organization classification. Patient samples were prepared after the research plan was approved by the Institutional Review Board at Hiroshima University, and written informed consent was obtained in accordance with the Declaration of Helsinki. Investigations were carried out in accordance with ethical standards authorized by the ethics committee of Hiroshima University and the ethics committee of the University of Tokyo (approval no. 20-10-0620)

Real-time RT-PCR

Total RNA was extracted from human bone marrow or peripheral blood cells using a TRIzol Kit (Invitrogen) according to the manufacturer's instructions, and converted to cDNA with a High Capacity cDNA Reverse Transcription Kit (Applied Biosystems). Total RNA of mouse progenitors was extracted with RNeasy (QIAGEN) according to the manufacturer's instructions, and converted to cDNA with a High Capacity cDNA Reverse Transcription Kit (Applied Biosystems). Real-time RT-PCR was performed using a LightCycler Workflow System (Roche Diagnostics). cDNA was amplified using a SYBR Premix EX Taq (Takara). Reaction was subjected to 1 cycle of 95°C for 30 seconds, 45 cycles of PCR at 95°C for 5 seconds, 58°C for 10 seconds, and 72°C for 10 seconds. All samples were independently analyzed at least 3 times. The following primer pairs were used: 5′-CCAGTTTGCTTTCCTCATTCC-3′ (forward) and 5′-TCTTCTCTCCCAGTATTCAAGTTCC-3′ (reverse) for human Hes1[22]; 5′-GAGCTGAACGGGAAGCTCACTGG-3′ (forward) and 5′-CAACTGTGAGGAGGGGAGATTCAG-3′ (reverse) for human GAPDH[22]; 5′-GAACAGCAACGAGTACCGGGTA-3′ (forward) and 5′-CCCATGGCCTTGACCAAGGAG-3′ (reverse) for mouse C/EBP-α[23]; 5′-CACAGGACTAGAACACCTGC-3′ (forward) and 5′-GCTGGTGAAAAGGACCTCT-3′ (reverse) for mouse hypoxanthine phosphoribosyltransferase (HPRT).[23] Relative gene expression levels were calculated using standard curves generated by serial dilutions of cDNA. Product quality was checked by melting curve analysis via LightCycler software (Roche Diagnostics). Expression levels were normalized by a control, the expression level of GAPDH mRNA for human samples, and HPRT mRNA for mouse samples.

Western blot analysis

To detect the expression of Hes1 or BCR-ABL (p210) proteins, equal numbers of cells from spleen or cell line were lysed, and Western blotting was performed as described with minor modifications.[24] Polyclonal rabbit anti-Hes1 antibody (H-140; Santa Cruz Biotechnology) and polyclonal rabbit anti–c-ABL antibody (K-12; Santa Cruz Biotechnology) were used for Hes1 or BCR-ABL detection, respectively.

Results

Retroviral transduction of Hes1 immortalizes CMPs and GMPs

NGFR-sorted Hes1-transduced KSLs, CMPs, and GMPs similarly generated compact and relatively large colonies, whereas empty vector-transduced KSLs generated a similar number of less large colonies. Empty vector-transduced CMPs and GMPs did not generate colonies (Figure 1A). Cytospin preparations of Hes1-transduced progenitors, stained with Hemacolor (Merck), showed blast-like morphologies, whereas those of empty vector-transduced KSLs contained bands, macrophages, and blasts (Figure 1B). Most of the empty vector-transduced CMPs and GMPs died and few cells remained (Figure 1B). In serial colony-forming assays, both CMPs and GMPs transduced with Hes1 formed colonies after at least 4 rounds of replating, with the plating efficiency more than 15% at the fourth round (Figure 1C). Replating could be reproducibly maintained for more than half a year, implying immortalizing activity of Hes1 (Figure 1D). The Hes1-transduced KSLs, CMPs, and GMPs were dependent on the presence of IL-3, requiring concentrations more than 1 ng/mL (Figure 1E; supplemental Figure 1A-B, available on the *Blood* website; see the Supplemental Materials link at the top of the online article). There was no significant difference between these cells in the dependency on IL-3. The majority of Hes1-transduced cells expressed c-Kit and CD34 at high levels, Sca-1 and CD11b at intermediate levels (Figure 1F, supplemental Figure 2A-B), irrespective of whether they were derived from KSLs, CMPs, or GMPs (supplemental Figure 2E).

The Lin$^-$ cells were further analyzed by adopting 5-color flow cytometry that is used to identify bone marrow KSLs, CMPs, and GMPs. The expression levels of c-Kit, Sca-1, and CD34 were distributed over wide ranges. Approximately 2.5% to 6.4% of all nucleated cells showed a phenotype similar to KSLs, and another 4.8% to 11.6% showed a phenotype similar to GMPs. There were few cells that resembled CMPs (Figure 1G). We sorted the KSL-like cells, CMP-like cells, and GMP-like cells from each Hes1-transduced cell (Hes1-KSLs, Hes1-CMPs, and Hes1-GMPs) and cultured them for a week in methylcellulose. The same analysis by 5-color flow cytometry showed accumulation of GMP-like cells (~ 45.3%-83.5% of all nucleated cells) and moderate accumulation of KSL-like cells (~ 4.3%-23.4% of all nucleated cells) in the cultured cells (supplemental Figure 3A-C).

BCR-ABL replaces IL-3 in Hes1-immortalized cell lines

Because the Hes1-immortalized cell lines were IL-3 dependent for their growth in vitro, we examined whether additional signaling could replace IL-3. IL-3 signaling takes place mainly via Stat-, Ras-MAPK-, and PI3K-Akt-dependent pathways. It is also known that CML-specific BCR-ABL (p210) can replace IL-3 signaling in several experimental designs. Thus, we retrovirally expressed BCR-ABL together with Hes1. The combination of Hes1 and BCR-ABL enabled KSLs, CMPs, and GMPs to form colonies after repeated replating, not only in the presence of cytokines (Figure 2A left panel) but also in the condition free from cytokines (Figure 2A right panel). In contrast, KSLs, but not CMPs or GMPs, formed colonies by BCR-ABL transduction alone only when supplemented with cytokines (Figure 2A left panel), and they did not form any colonies without cytokines (Figure 2A right panel) or after replating with/without cytokines (Figure 2A both panels). In the liquid culture, it was shown that KSLs, CMPs, and GMPs transduced with both Hes1 and BCR-ABL were immortalized without cytokine supplementation (Figure 2B). The colonies made from Hes1- and BCR-ABL-transduced cells showed similar morphology with those from Hes1-transduced cells in the presence of a cytokine cocktail (Figure 2C). Importantly, the morphology of colony-forming cells derived from BCR-ABL-transduced KSLs was much more mature compared with those derived from Hes1- and BCR-ABL-transduced KSLs, CMPs, and GMPs, even in the same cytokine cocktail (Figure 2D). The majority of Hes1$^+$BCR-ABL$^+$ KSLs as well as Hes1$^+$BCR-ABL$^+$ CMPs and GMPs expressed CD34 at high levels, whereas they expressed c-Kit, Sca-1, and CD11b at intermediate levels (Figure 2E; supplemental Figure 2C-D), irrespective of whether they were derived from

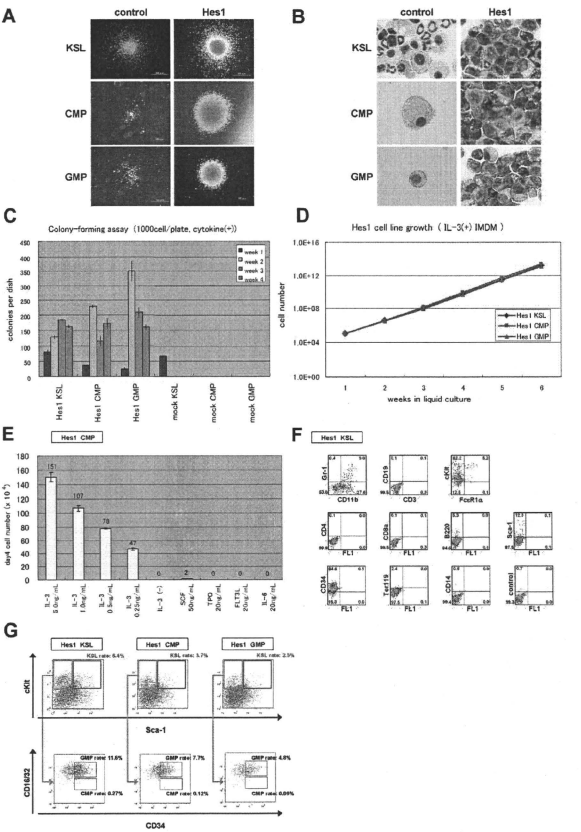

Figure 1. Hes1-transduced KSLs, CMPs, or GMPs were immortalized in the presence of IL-3. (A) Typical colonies derived from Hes1- and empty vector-transduced KSLs, CMPs, and GMPs in the presence of SCF, TPO, IL-3, and IL-6. Images were obtained with an IX70 microscope and a DP70 camera (Olympus); an objective lens, UPlanFI (Olympus); original magnification ×40 (bottom 2 in the right panels) and original magnification ×100 (remaining 4 panels). (B) Giemsa staining of Hes1- and control vector-transduced KSLs, CMPs, and GMPs. Images were obtained with a BX51 microscope and a DP12 camera (Olympus); an objective lens, UPlanFI (Olympus); original magnification ×1000. (C) Colony-forming assay from KSLs, CMPs, and GMPs transduced with Hes1 or empty vector. Hes1-transduced cells were replatable more than 4 times in vitro. Bars represent the number of colonies obtained per 10^3 cells after each round of plating in methylcellulose supplemented with SCF, TPO, IL-3, and IL-6. A representative result from 3 independent and reproducible experiments is shown. Error bars represent the SD from duplicate cultures. (D) Sustained growth of Hes1-transduced cells in liquid culture supplemented with 1 ng/mL IL-3. The number of cells was determined every 7 days by trypan blue staining, and 10^5 cells per well were seeded into a 6-well plate. Liquid culture was reproducibly continued for more than 6 months. (E) Cytokine requirement of Hes1-transduced CMPs. The cells were cultured in Iscove modified Dulbecco medium supplemented with indicated cytokines in duplicate. The numbers of cells were counted after 4 days of culture. A representative result from 2 independent and reproducible experiments is shown. Error bars represent the SD from duplicate cultures. Hes1-transduced KSLs and GMPs showed similar results (supplemental Figure 1A-B). (F) Flow-cytometric analysis of Hes1-transduced KSLs cultured in methylcellulose supplemented with SCF, TPO, IL-3, and IL-6. The dot plots represent Gr-1, CD19, c-Kit, CD4, CD8a, B220, Sca-1, CD34, Ter119, and CD14 labeled with a corresponding PE-conjugated monoclonal antibody versus CD11b, CD3, and FcεR1α labeled with a corresponding fluorescein isothiocyanate-conjugated monoclonal antibody or FL1 with no monoclonal antibody. Hes1-transduced CMPs and GMPs showed similar expression patterns (supplemental Figure 2A-B). (G) Flow-cytometric analysis of Lin$^-$-gated Hes1-transduced cells. Five-color analyses are used to identify KSL-like (top panels) and CMP-like and GMP-like cells (bottom panels) in the Hes1-transduced KSLs, CMPs, and GMPs. The number shows the percentage of cells in all nucleated cells. The analyzed cells were NGFR sorted at 48 to 60 hours from the initiation of Hes1- or control vector-transduction and cultured for the following lengths of time before the analysis: (A) 1 week, (B) 1 week, (C) 0 days, (D) 4 weeks, (E) 2 weeks, (F) 1 week, and (E) 2 weeks.

KSLs, CMPs, or GMPs (supplemental Figure 2F). Hes1$^+$BCR-ABL$^+$ KSLs, CMPs, and GMPs showed lower expressions of c-Kit and CD34 than KSLs, CMPs, and GMPs transduced with Hes1 alone (supplemental Figure 2E-F) when cultured in the presence of the same cytokine cocktail (SCF, TPO, IL-3, and IL-6). Expression of Hes1 or BCR-ABL in the Hes1 ± BCR-ABL transduced CMP or GMP cell lines was confirmed by Western blot analysis (supplemental Figure 4A).

Hes1$^+$BCR-ABL$^+$ CMPs and GMPs rapidly induce AML/CML blast crisis-like disease in recipient mice

To examine the effect of Hes1 on leukemogenesis, Hes1-transduced KSLs, CMPs, and GMPs were injected through tail veins into C57BL/6-Ly5.2 recipient mice (8-12 weeks of age) after a sublethal (5.25 Gy) or a lethal (9.5 Gy) dose of total-body γ-irradiation (^{135}Cs). For the lethally irradiated mice, 2×10^5 bone marrow cells from C57BL/6-Ly5.2 mice were simultaneously injected for radioprotection. All the mice that received transplantations of Hes1-transduced KSLs, CMPs, and GMPs were kept healthy, and no recipients developed myeloproliferative neoplasms (MPNs) or leukemias for up to 250 days after the transplantation (Figure 3A). Regarding the nonleukemogenic nature of the stem/progenitor cells transduced with Hes1 alone, we[7] and others[25] previously reported similar results, although the cell populations and/or experimental designs were not identical.

In agreement with the previous reports,[26] recipient mice injected with BCR-ABL-transduced KSLs developed fatal MPN within 30 days after the transplantation, whereas those injected with BCR-ABL-transduced CMPs and GMPs were kept healthy for more than 130 days. We did not find any signs of MPN or leukemias when mice were killed between 130 and 200 days after the transplantation (Figure 3B).

Because we found that the combination of Hes1 and BCR-ABL transduction conferred cytokine-independent immortalization on CMPs and GMPs, we injected Hes1$^+$BCR-ABL$^+$ KSLs, CMPs, and GMPs through tail veins into C57BL/6-Ly5.2 recipient mice

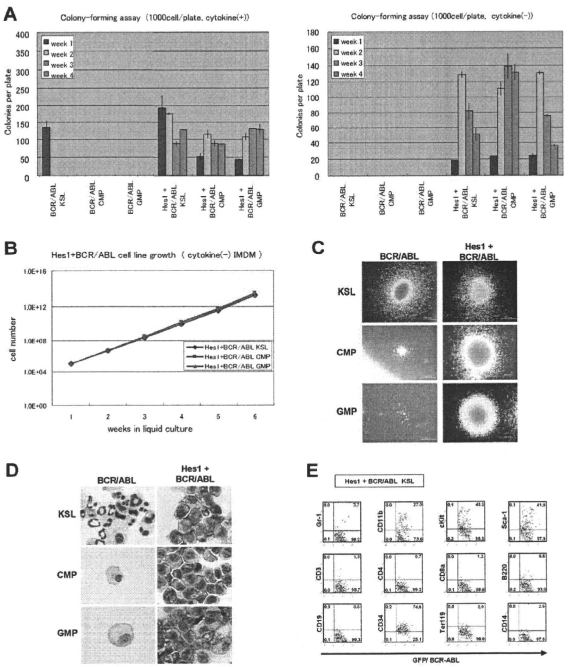

Figure 2. Hes1- and BCR-ABL-transduced KSLs, CMPs, or GMPs were immortalized independently of IL-3. (A) Colony-forming assay of KSLs, CMPs, and GMPs transduced with BCR-ABL alone or Hes1 and BCR-ABL, cultured in methylcellulose with or without cytokine cocktail containing SCF, TPO, IL-3, and IL-6. Hes1^{-}BCR-ABL^{+} cells could be serially replated more than 4 times both with or without cytokines. In contrast, whereas KSLs, but not CMPs or GMPs, transduced with BCR-ABL alone, formed colonies in the presence of cytokines, neither KSLs, nor CMPs, nor GMPs formed colonies without cytokine supplementation. Bars represent the number of colonies obtained per 10^5 cells after each round of plating in methylcellulose. A representative result from 3 independent and reproducible experiments is shown. Error bars represent the SD from duplicate cultures. (B) Sustained growth of Hes1^{+}BCR-ABL^{+} cells in liquid culture without cytokine supplementation. The numbers of cells were determined every 7 days by trypan blue staining, and 10^5 cells per well were seeded into a 6-well plate. Liquid culture was reproducibly continued for more than 6 months. (C) Typical colonies derived from KSLs, CMPs, and GMPs transduced with BCR-ABL alone (left panels) or BCR-ABL and Hes1 (right panels) in the presence of SCF, TPO, IL-3, and IL-6. Images were obtained with an IX70 microscope and a DP70 camera (Olympus); an objective lens, UPlanFl (Olympus); original magnification ×100. (D) Giemsa staining of Hes1^{+}BCR-ABL^{+} KSLs, CMPs, and GMPs. Images were obtained with a BX51 microscope and a DP12 camera (Olympus); an objective lens, UPlanFl (Olympus); original magnification ×1000. (E) Flow-cytometric analysis of Hes1^{+}BCR-ABL^{+} KSLs cultured in methylcellulose supplemented with SCF, TPO, IL-3, and IL-6. The dot plots represent Gr-1, CD11b, c-Kit, Sca-1, CD3, CD4, CD8a, B220, CD19, CD34, Ter119, and CD14 labeled with a corresponding PE-conjugated monoclonal antibody versus expression of GFP/BCR-ABL. Hes1^{+}BCR-ABL^{+} CMPs and GMPs showed a similar expression pattern (supplemental Figure 2C-D). The analyzed cells were GFP and NGFR sorted at 48 to 60 hours from the initiation of BCR-ABL- or Hes1 + BCR-ABL transduction and cultured for the following lengths of time before the analysis: (A) 0 days, (B) 4 weeks, (C) 1 week, (D) 1 week, and (E) 1 week.

after sublethal irradiation. The numbers of cells injected varied among experiments, ranging from 17×10^2 to 15×10^4, because of the difference in sorting efficiencies. All the mice receiving transplantations rapidly developed fatal AML/CML in blast crisis-like disease with no significant difference in latency, ranging between 18 and 39 days after the transplantation ($P < .867$) (Figure 4A). The tissue distribution of the disease was virtually the same among mice receiving KSLs, CMPs, and GMPs; they invariably demonstrated marked hepatosplenomegaly and lung hemorrhage resulting from infiltration of leukemic cells (Figure 4B). Expression of Hes1 and BCR-ABL in the spleen cells of recipient mice was confirmed by Western blot analysis (supplemental Figure 4B).

The morphology of bone marrow demonstrated increased myeloid blasts (Figure 4C), and the histology of spleen, liver, and lungs demonstrated extensive infiltration of leukemic cells (Figure 4D). The percentages of the blasts ranged between 28% and 55% of all nucleated bone marrow cells (mean, 36.5%) of the mice receiving Hes1- and BCR-ABL-transduced KSLs, CMPs, and GMPs. In contrast, the percentages of bone marrow blasts in the recipient mice receiving BCR-ABL-transduced KSLs were only 6% to 7% (Figure 5A). White blood cell counts in the peripheral blood of recipients with Hes1^{+}BCR-ABL^{+} KSLs, CMPs, and GMPs were $2.4 \times 10^4/\mu L$ to $67.9 \times 10^4/\mu L$ (mean, $17.8 \times 10^4/\mu L$), whereas those with BCR-ABL-transduced KSLs showed moderate leukocytosis ranging between $2.9 \times 10^4/\mu L$ and $3.8 \times 10^4/\mu L$ (Figure 5B). The surface marker profiles of the bone marrow cells from the recipients with Hes1^{+}BCR-ABL^{+} cells expressed CD11b and Gr-1 at high levels, whereas they expressed c-Kit, Sca-1, and CD34 at intermediate levels (Figure 5C; supplemental Figure 5A-B), irrespective of whether they were derived from KSLs, CMPs, or GMPs (supplemental Figure 5C).

The long-term self-renewal properties of the leukemic cells derived from Hes1- and BCR-ABL-transduced CMPs or GMPs were tested by transplantation into secondary recipients; 0.1 to 5×10^6 total bone marrow cells were injected into the tail veins of sublethally irradiated mice. All recipient mice transplanted with more than 10^5 Hes1^{+} cells from bone marrow developed fatal AML/CML in blast crisis-like disease with latencies of between 18 and 75 days (supplemental Figure 4C). The disease was almost identical with the primary disease (data not shown).

Hes1 expression is elevated in a substantial subset of human CML blast crisis samples

The results presented from the mouse model experiments suggest a potential link between deregulated expression of Hes1 and human CML in blast crisis. We measured the Hes1 mRNA by real-time RT-PCR in 11 peripheral blood, 1 cerebrospinal fluid, and 8 bone marrow samples from CML in blast crisis patients; 19 bone marrow samples from CML in chronic phase patients; and 10 bone marrow samples from normal subjects. In 8 of 20 CML in blast crisis samples, we found that Hes1 mRNA levels were elevated by more than 4 times the average of normal bone marrow samples (Figure

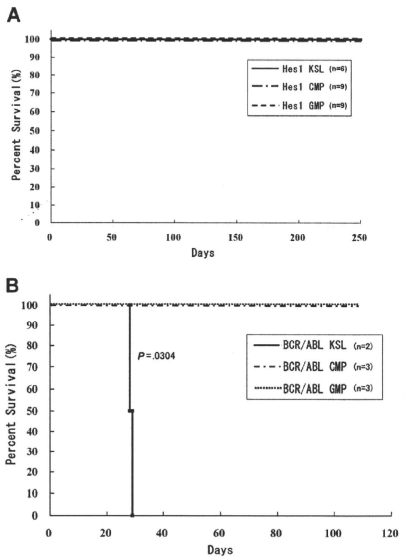

Figure 3. Mice transplanted with Hes1-transduced KSLs, CMPs, and GMPs were kept healthy. (A) Survival curves for mice injected with Hes1-transduced progenitors. No mice showed any signs of MPN for more than 250 days from transplantation. Data were analyzed by the Kaplan-Meier method. The numbers of transplanted mice are shown. Three independent experiments were performed. (B) Survival curves for mice injected with BCR-ABL-transduced progenitors. Mice transplanted with BCR-ABL-transduced KSLs developed fatal MPN within 30 days after transplantation, whereas mice transplanted with BCR-ABL-transduced CMPs or GMPs showed no evidence of disease when killed between 130 and 200 days after transplantation. Data were analyzed using the log-rank test. The 2 independent experiments were performed, and the total numbers of transplanted mice are shown.

6A). Interestingly, all but one of their phenotypes were myeloid, and 5 of 12 samples in which Hes1 mRNA levels were not elevated were derived from patients with B-cell lineage lymphoid crisis. On the other hand, the average of Hes1 mRNA levels in CML in chronic phase samples seemed to be lower than that of the normal bone marrow samples, with no sample exceeding twice the average. Clinical data of 20 patients with CML in blast crisis are shown in Table 1. The correlation coefficient between the blast percentage and the Hes1 mRNA level was −0.395, indicating that the elevated Hes1 expression level was independent of the increase in the blast percentage.

To investigate the role of Hes1 in CML blast crisis, we measured the Hes1 mRNA by real-time RT-PCR in 5 human cell lines (K-562,[27] JK-1,[28] KCL-22,[29] TS9:22,[30] and JURL-MK1[31]), which were derived from CML in blast crisis. We found that, in 3 of 5 CML blast crisis cell lines, Hes1 mRNA levels were elevated compared with the normal bone marrow sample (Figure 6B). We transduced a dominant-negative Hes1 (dnHes1) lacking a C-terminal WRPW domain via retrovirus vector into the 3 cell lines (K-562, TS9:22, and JURL-MK1) in which Hes1 mRNA levels were elevated. Indeed, in 2 of these 3 cell lines, proliferation was significantly suppressed by transduction of dnHes1 (Figure 6C). The repression of C/EBP-α by Hes1 was also observed in Hes1-transduced KSLs, CMPs, and GMPs compared with control vector-transduced KSLs, CMPs, and GMPs (Figure 6D). When C/EBP-α retrovirus vector was transduced to Hes1-transduced KSLs, CMPs, and GMPs, all of these cells differentiated to segmented neutrophils, suggesting that the expression of C/EBP-α reversed the function of Hes1 (supplemental Figure 6).

Discussion

In the present study, we demonstrated that retroviral transduction of Hes1 readily immortalizes myeloid progenitors at various stages.

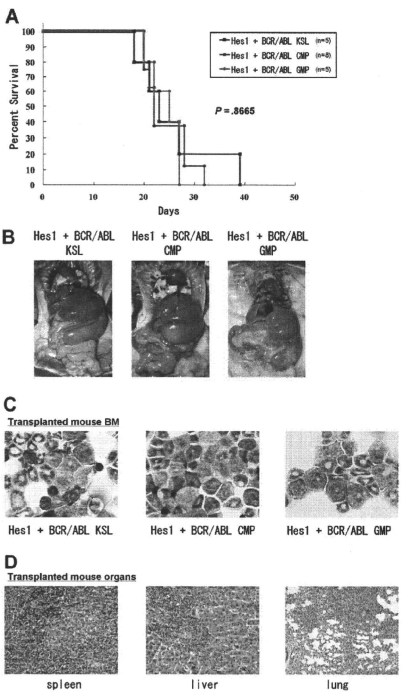

Figure 4. CMPs and GMPs transduced with the combination of Hes1 and BCR-ABL rapidly induced AML/blast crisis of CML. (A) Survival curves of mice. KSLs (n = 5), CMPs (n = 8), and GMPs (n = 5) transduced with the combination of Hes1 and BCR-ABL developed fatal AML/CML in blast crisis-like disease within 18 to 39 days, 20 to 32 days, and 20 to 27 days, respectively. Numbers of injected cells ranged 17×10^2 to 2.6×10^4 for KSLs, 5.5×10^4 to 15×10^4 for CMPs, and 4.0×10^4 to 13.8×10^4 for GMPs. There was no significant difference in latency of penetrance ($P < .867$). Statistical differences were determined using the log-rank test. Three independent experiments were performed, and the total numbers of transplanted mice are shown. (B) Tissue distribution of the leukemic cells. Mice transplanted with KSLs, CMPs, and GMPs transduced with the combination of Hes1 and BCR-ABL invariably demonstrated marked hepatosplenomegaly and lung hemorrhage, both resulting from infiltration of leukemic cells. (C) The morphology of bone marrow cells from representative recipient mice. Increased myeloid blasts were seen with no significant difference among KSLs, CMPs, and GMPs. (D) Histology of spleen, liver, and lungs from representative mice receiving Hes1$^+$BCR-ABL$^+$ GMPs. Vast infiltration of leukemic cells is seen. There were no differences in the histology among mice receiving Hes1$^+$BCR-ABL$^+$ KSLs, CMPs, and GMPs.

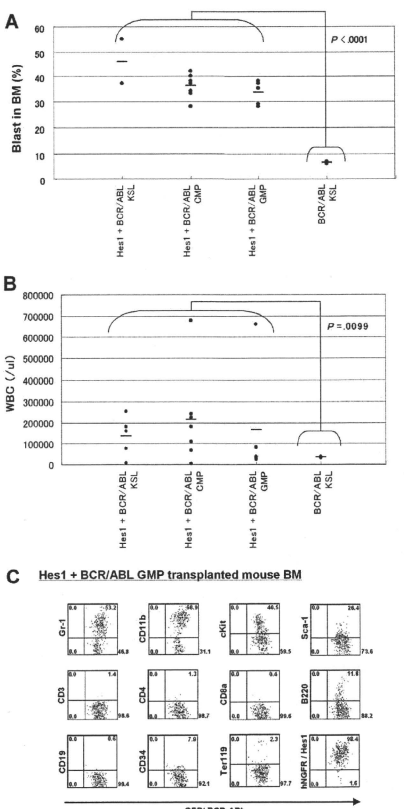

Figure 5. Comparisons of blast percentages in the bone marrow and peripheral blood leukocyte counts between mice receiving KSLs transduced with BCR-ABL alone and those receiving KSLs, CMPs, and GMPs transduced with the combination of Hes1 and BCR-ABL. (A) Blast ratios in the bone marrow. The mean blast ratios in all nucleated bone marrow cells were 6.5% ± 0.7% and 36.5% ± 6.9% in mice receiving KSLs transduced with BCR-ABL alone and in those receiving KSLs, CMPs, and GMPs transduced with the combination of Hes1 and BCR-ABL, respectively. The difference was statistically significant by the 2-sample *t* test with Welch correction ($P < .001$). (B) Peripheral white blood cell counts (WBCs). WBCs were $3.4 \pm 0.6 \times 10^4/\mu L$ and $17.8 \pm 20.3 \times 10^4/\mu L$ in mice receiving KSLs transduced with BCR-ABL alone and in those receiving KSLs, CMPs, and GMPs transduced with the combination of Hes1 and BCR-ABL, respectively. The difference was statistically significant by the 2-sample *t* test with Welch correction ($P < .001$). (C) Flow-cytometric analysis of bone marrow cells from mice receiving GMPs transduced with the combination of Hes1 and BCR-ABL. The dot plots represent Gr-1, CD11b, c-Kit, Sca-1, CD3, CD4, CD8a, B220, CD19, CD34, Ter119, and NGFR labeled with the corresponding PE-conjugated monoclonal antibody versus expression of GFP/BCR-ABL. NGFR is a marker of Hes1, and GFP is a marker of BCR-ABL transduction. The bone marrow cells derived from mice receiving KSLs or CMPs transduced with the combination of Hes1 and BCR-ABL showed essentially the same pattern (supplemental Figure 5A-B).

Moreover, when BCR-ABL is transduced together, Hes1 tranforms differentiated myeloid progenitors, such as CMPs and GMPs, in addition to hematopoietic stem cell-rich population, such as KSLs, to AML/CML in blast crisis-like cells, rapidly killing recipient mice. This result is in sharp contrast to the fact that a hematopoietic stem cell-containing population is required for BCR-ABL to cause MPN-like disease.

Hes1 is known as an effector molecule functioning downstream of Notch signaling. The activating mutations of the extracellular heterodimerization domain and/or the C-terminal PEST domain of Notch1 have been identified in approximately 50% of human T-cell acute lymphoblastic leukemias.[10,32] We have recently identified gain-of-function mutations of *Notch2* in conjunction with increased copy numbers of the mutation-carrying *Notch2* allele in a subset of B-cell lymphomas.[11] A possible association between deregulated Notch signaling is also reported in Hodgkin lymphoma, anaplastic large cell lymphoma, small-cell lung cancer, and prostate adenocarcinoma, etc.[33] Regarding myeloid malignancies, however, only one paper reports the identification of the activating mutation of Notch1 in 1 of 12 human AML samples.[34] Given that Notch signaling is among the strongest inducers of T-cell lineage commitment[12,13] and that increased Notch signaling could block myeloid lineage commitment,[15] deregulated Notch signaling might antagonize, rather than promote, the development of myeloid malignancies. However, Hes1 does not necessarily represent Notch signaling. Indeed, other extracellular signaling, such as Sonic Hedgehog,[35] could affect Hes1 expression, and cross-talk between Hes family proteins and molecules in various cell signaling pathways, such as Stat3,[36] has been demonstrated.

We previously reported that Hes1 preserved highly purified hematopoietic stem cells in vitro and contributed to the expansion of transduced hematopoietic stem cells in the recipients' bone marrow,[7] but the effect of Hes1 transduction on myeloid progenitors was not evaluated in detail. We have now found the myeloid progenitor-immortalizing activity of Hes1. In addition, accumulation of KSL- and GMP-like population in Hes1-transduced cells implicates a role for Hes1 in leukemic stem cells. On the other hand, we have also found that the in vitro growth of the Hes1-immortalized cells is dependent on cytokine signaling and that Hes1 alone is insufficient to be fully leukemogenic when overexpressed. The mainstay of the Hes1 effects on myeloid progenitors appears to be blockade of differentiation, although other functions, such as reversion from the quiescent state to the actively cycling state,[21] may also be involved. In the present study, we confirmed that Hes1 expression represses C/EBP-α, a transcription factor having important roles in myeloid differentiation, in mouse KSLs and committed progenitors as we reported.[15] Moreover, transduction of C/EBP-α reversed the differentiation block caused by Hes1 expression, which partially explains the mechanism of blocked myeloid differentiation by Hes1. C/EBP-α is frequently mutated in AML with the normal karyotype.[37-39] In other human AML without C/EBP-α mutations, reduced C/EBP-α expression, possibly through deregulated epigenetic control, is not uncommon and is associated with poor prognosis.[40,41] Furthermore, mice injected with mutated C/EBP-α-transduced bone marrow cells develop myelodysplastic syndrome and AML.[42] Therefore, reduction of C/EBP-α function is highly relevant to the development and/or progression of myeloid malignancies. Hes1, therefore, might be involved in human myeloid malignancies through suppression of C/EBP-α.

Up-regulation of Hes1 is shown in a subset of human rhabdomyosarcomas[21] and medulloblastomas.[43,44] In the present study, we have detected elevated expression of Hes1 in 8 of the 20 samples from CML in blast crisis patients, but not those from CML

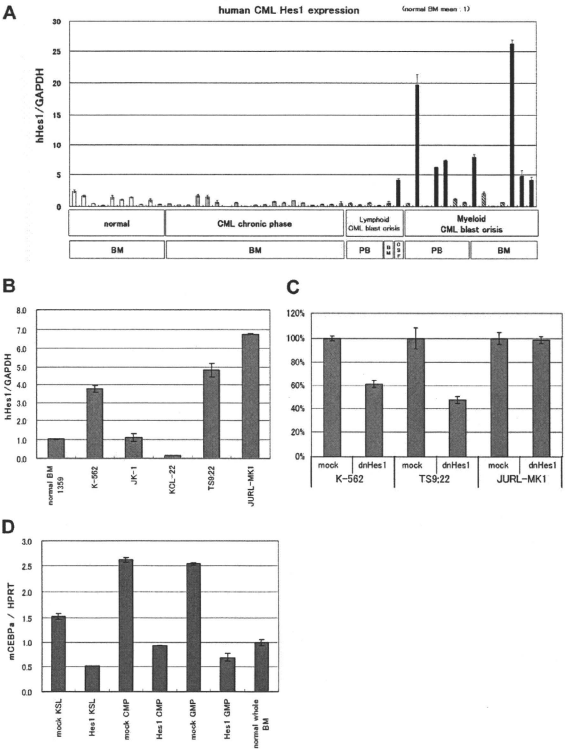

Figure 6. Hes1 expression was elevated in approximately 40% of patients with CML in blast crisis. (A) Real-time RT-PCR for Hes1 in bone marrow or peripheral blood cells from healthy subjects, patients with CML in chronic phase, or patients with CML in blast crisis. Expression levels were normalized by GAPDH mRNA. RNA from normal bone marrow cells served as a control (mean of 10 RNA levels of normal bone marrow was defined as 1). Hes1 mRNA levels exceeded 4 (solid bar) in 8 of 20 samples from CML in blast crisis patients. The correlation coefficient determined by the Wilcoxon signed-rank test between blast ratio and Hes1-expression level was −0.395. PB indicates peripheral blood; BM, bone marrow; CSF, cerebrospinal fluid. The solid bar represents CML in blast crisis exceeding 4; the hatched bar represents CML in blast crisis less than 4. (B) Hes1 expression in 5 human CML blast crisis cell lines. Expression levels of HES1 in K-562, JK-1, KCL-22, TS9:22, and JURL-MK1 were evaluated by real-time RT-PCR and were normalized by GAPDH mRNA. (C) Growth repression by transduction of dnHes1 (a dominant-negative Hes1) retrovirus vector into 3 human cell lines (K-562, TS9:22, and JURL-MK1). Six days after retrovirus transduction, cell numbers were counted. Growth is shown as a percentage of the control cells that were transduced with control vector. A representative result from 2 independent and reproducible experiments is shown. Error bars represent the SD from duplicate cultures. (D) Real-time RT-PCR for C/EBP-α in Hes1-transduced KSLs, CMPs, and GMPs compared with control vector-transduced KSLs, CMPs and GMPs. Total RNA was extracted at 60 hours from the initiation of Hes1-transduction. Error bars represent the SD from 2 independent experiments in (A-B,D).

in chronic phase patients. Although it is yet to be confirmed by a larger number of samples from CML as well as AML patients, this result indicates an interesting connection between the mouse model of AML/CML in blast crisis-like disease and human leukemia. In addition, we have demonstrated that transduction of dnHes1 represses the proliferation in 2 of 3 human cell lines of CML in blast crisis. These results suggest that Hes1 plays an important role in blast crisis of CML.

Although the origin of CML is considered to be a hematopoietic stem cell, blast crisis has been shown to be a result of transformation of myeloid progenitors.[16] BCR-ABL can cause MPN-like disease when introduced into the hematopoietic stem cell population but cannot induce MPN or leukemia when introduced into differentiated myeloid progenitors.[26] Therefore, development of full-blown AML/CML in blast crisis-like disease in mice with differentiated progenitors only by cotransduction with Hes1 and BCR-ABL may represent a true model of blast crisis of CML. In this context, Hes1 is a possible crisis-promoting gene like other examples, such as activated β-catenin[16] and BCL-2,[45] both of which caused CML in blast crisis-like disease in mice when transduced into GMPs together with BCR-ABL.

Several AML-associated fusion gene products, such as MLL-ENL,[46] MOZ-TIF2,[26] and MLL-AF9,[47] have been demonstrated to confer replating capacity on CMPs and GMPs, and eventually to transform these cells into leukemia-initiating cells. Unique to our findings is the fact that we transduced a wild-type transcription factor, Hes1, and found that such simple up-regulation of a transcription factor led to similar transformation phenotypes. A substantial number of examples have indicated that loss of function or altered function, rather than gain of function, of transcription factors, including MLL, MOZ, Runx1, RARα, C/EBP-α, etc, is associated with leukemogenesis. If up-regulation of Hes1 is indeed involved in human leukemias, this represents a new mechanism of leukemogenesis.

In modeling CML in mice, the present model provides a powerful tool by which we can induce 2 distinct phases of CML from stem cells or progenitors using BCR-ABL gene: a chronic phase-like state by transduction of KSL with BCR-ABL alone and a blast crisis-like state by cotransduction of CMPs and GMPs with BCR-ABL and Hes1.

In conclusion, we have developed a useful mouse model for CML blast crisis and have indicated that Hes1 is a key molecule in blast crisis transition in CML. The present mouse model will aid

Table 1. Clinical data of 20 patients with CML in blast crisis

Sample name	Source	Blast ratio	Hes1/GAPDH	Phenotype	Chromosome aberration	Clinical features
228 CML BC	PB	57	0.49	B-ALL	46,XY,t(9;22)/46,XY, +der(1;14)(q10;q12),t(9;22)	—
428 CML BC	PB	100	0.27	B-ALL	t(9;22)	—
984 CML BC	PB	60	0.56	B-ALL	46, XX, t(9;22)(q34;q11.2)	—
3259 CML BC	PB	100	0.16	B-ALL	t(9;22)	—
1385 CML BC	BM	81	0.56	B-ALL	t(9;22)	—
1107 CML BC	CSF	100	4.16	B-ALL	t(9;22)	The blasts increased drastically in CNS.
1 CML BC	PB	90	0.51	Myeloid	t(9;22)	—
219 CML BC	PB	12	19.72	Myeloid	45,XX,-7,t(9;22)	BM was dry tap composed of 100% blasts.
393 CML BC	PB	20	0.08	Myeloid	46,XX,t(9;22),add(17)(p11)	—
1088 CML BC	PB	30	6.22	Myeloid	46, XX, t(9;22)(q34;q11.2)	BM was dry tap.
1299 CML BC	PB	20	7.35	Myeloid	t(9;22)	BM was dry tap composed of 23% blasts.
1824 CML BC	PB	51	1.15	Myeloid	t(9;22)	BM was dry tap.
3153 CML BC	PB	7	0.66	Myeloid	t(9;22)	BM was dry tap. The blasts in BM increased up to 42% after taking this sample.
232 CML BC	BM	11	7.96	Myeloid	47,XY, +8,t(9;22)	The blasts in BM increased drastically up to 44% after taking this sample.
452 CML BC	BM	54	2.01	Myeloid	46,dic(17)(q10),t(9;22)	—
916 CML BC	BM	24	0.11	Myeloid	t(9;22)	—
1091 CML BC	BM	28	0.67	Myeloid	t(9;22)	—
811 CML BC	BM	25	26.25	Myeloid	46, XX, t(1;9;22)(q44;q34;q11.2)	—
3332 CML BC	BM	22	4.17	Myeloid	t(9;22)	—
3847 CML BC	BM	62	4.79	Myeloid	t(9;22)	—

CML indicates chronic myelogenous leukemia; BC, blast crisis; PB, peripheral blood; B-ALL, B-cell acute lymphoblastic leukemia; BM, bone marrow; CSF, cerebrospinal fluid; —, not applicable; and CNS, central nervous system.

understanding of the molecular mechanisms underlying blast crisis of CML and might lead to a better therapeutic outcome for this difficult disease.

Acknowledgments

The authors thank Dr R. Kageyama for the Hes1 cDNA; Dr H. Nakauchi and Dr M. Onodera for the GCDNsam/IRES-NGFR vector and the GCDNsam/IRES-GFP vector; Dr K. Akashi and Dr S. Mizuno for mouse C/EBP-α cDNA; Dr T. Inaba and Dr H. Asou (Hiroshima University, Hiroshima, Japan) for the JK-1, KCL-22, JURL-MK1 cell line; and Kirin Pharma for the TPO.

This work was supported by a Grant-in-Aid for Scientific Research (KAKENHI no. 20249051) and the Global Center of Excellence Program Center of Education and Research for the Advanced Genome-Based Medicine (for personalized medicine and the control of worldwide infectious diseases); the Ministry of Education, Culture, Sports, Science, and Technology of Japan (MEXT) and the Ministry of Health and Welfare of Japan (T.K.); and KAKENHI (no. 19390258), Astellas Foundation for Research on Metabolic Disorders, Uehara Memorial Foundation, and Princess Takamatsu Cancer Research Fund (S.C.).

Authorship

Contribution: F.N. did all the experiments and participated actively in writing the manuscript; M.S.-Y. and J.K. assisted with the experiments and actively participated in designing the experiments; Y.K., N.K., T.U., K.H., and K.K. assisted with the experiments; Y.H. and H.H. provided human samples; S.O. and M.K. participated in interpretation and designing the experiments; and T.K. and S.C. conceived the project, secured funding, and actively participated in manuscript writing.

Conflict-of-interest disclosure: T.K. serves as a consultant for R&D Systems and Rigel Pharmaceuticals. The remaining authors declare no competing financial interests.

Correspondence: Toshio Kitamura, Division of Stem Cell Signaling, Center for Stem Cell Therapy, Institute of Medical Science, University of Tokyo, 4-6-1 Shirokanedai, Minato-ku, Tokyo 108-8639, Japan; e-mail: kitamura@ims.u-tokyo.ac.jp; and Shigeru Chiba, Department of Hematology, Graduate School of Comprehensive Human Sciences, University of Tsukuba, 1-1-1 Tennodai, Tsukuba, Ibaraki 305-8575, Japan; e-mail: schiba-tky@umin.net.

References

1. Kageyama R, Nakanishi S. Helix-loop-helix factors in growth and differentiation of the vertebrate nervous system. *Curr Opin Genet Dev.* 1997;7(5):659-665.
2. Jarriault S, Brou C, Logeat F, Schroeter EH, Kopan R, Israel A. Signalling downstream of activated mammalian Notch. *Nature.* 1995;377(6547):355-358.
3. Jarriault S, Le Bail O, Hirsinger E, et al. Delta-1 activation of notch-1 signaling results in HES-1 transactivation. *Mol Cell Biol.* 1998;18(12):7423-7431.
4. Johnson JE, Birren SJ, Anderson DJ. Two rat homologues of Drosophila achaete-scute specifically expressed in neuronal precursors. *Nature.* 1990;346(6287):858-861.
5. Sumazaki R, Shiojiri N, Isoyama S, et al. Conversion of biliary system to pancreatic tissue in Hes1-deficient mice. *Nat Genet.* 2004;36(1):83-87.
6. Kumano K, Chiba S, Shimizu K, et al. Notch1 inhibits differentiation of hematopoietic cells by sustaining GATA-2 expression. *Blood.* 2001;98(12):3283-3289.
7. Kunisato A, Chiba S, Nakagami-Yamaguchi E, et al. HES-1 preserves purified hematopoietic stem cells ex vivo and accumulates side population cells in vivo. *Blood.* 2003;101(5):1777-1783.
8. Kaneta M, Osawa M, Sudo K, Nakauchi H, Farr AG, Takahama Y. A role for pref-1 and HES-1 in thymocyte development. *J Immunol.* 2000;164(1):256-264.
9. Tomita K, Hattori M, Nakamura E, Nakanishi S, Minato N, Kageyama R. The bHLH gene Hes1 is essential for expansion of early T cell precursors. *Genes Dev.* 1999;13(9):1203-1210.
10. Weng AP, Ferrando AA, Lee W, et al. Activating mutations of NOTCH1 in human T cell acute lymphoblastic leukemia. *Science.* 2004;306(5694):269-271.
11. Lee S-y, Kumano K, Nakazaki K, et al. Gain-of-function mutations and copy number increases of

Notch2 in diffuse large B-cell lymphoma. *Cancer Sci.* 2009;100(5):920-926.

12. Radtke F, Wilson A, Mancini SJ, MacDonald HR. Notch regulation of lymphocyte development and function. *Nat Immunol.* 2004;5(3):247-253.
13. Allman D, Punt JA, Izon DJ, Aster JC, Pear WS. An invitation to T and more: notch signaling in lymphopoiesis. *Cell.* 2002;109[suppl]:S1-S11.
14. Radtke F, Wilson A, Stark G, et al. Deficient T cell fate specification in mice with an induced inactivation of Notch1. *Immunity.* 1999;10(5):547-558.
15. Sakata-Yanagimoto M, Nakagami-Yamaguchi E, Saito T, et al. Coordinated regulation of transcription factors through Notch2 is an important mediator of mast cell fate. *Proc Natl Acad Sci U S A.* 2008;105(22):7839-7844.
16. Jamieson CH, Ailles LE, Dylla SJ, et al. Granulocyte-macrophage progenitors as candidate leukemic stem cells in blast-crisis CML. *N Engl J Med.* 2004; 351(7):657-667.
17. Akashi K, Traver D, Miyamoto T, Weissman IL. A clonogenic common myeloid progenitor that gives rise to all myeloid lineages. *Nature.* 2000; 404(6774):193-197.
18. Honda H, Fujii T, Takatoku M, et al. Expression of p210bcr/abl by metallothionein promoter induced T-cell leukemia in transgenic mice. *Blood.* 1995; 85(10):2853-2861.
19. Kitamura T, Koshino Y, Shibata F, et al. Retrovirus-mediated gene transfer and expression cloning: powerful tools in functional genomics. *Exp Hematol.* 2003;31(11):1007-1014.
20. Morita S, Kojima T, Kitamura T. Plat-E: an efficient and stable system for transient packaging of retroviruses. *Gene Ther.* 2000;7(12):1063-1066.
21. Sang L, Coller HA, Roberts JM. Control of the reversibility of cellular quiescence by the transcriptional repressor HES1. *Science.* 2008; 321(5892):1095-1100.
22. Hopfer O, Zwahlen D, Fey MF, Aebi S. The Notch pathway in ovarian carcinomas and adenomas. *Br J Cancer.* 2005;93(6):709-718.
23. Iwasaki H, Mizuno S, Mayfield R, et al. Identification of eosinophil lineage-committed progenitors in the murine bone marrow. *J Exp Med.* 2005; 201(12):1891-1897.
24. Ono R, Nakajima H, Ozaki K, et al. Dimerization of MLL fusion proteins and FLT3 activation synergize to induce multiple-lineage leukemogenesis. *J Clin Invest.* 2005;115(4):919-929.
25. Kawamata S, Du C, Li K, Lavau C. Overexpression of the Notch target genes Hes in vivo induces lymphoid and myeloid alterations. *Oncogene.* 2002;21(24):3855-3863.
26. Huntly BJ, Shigematsu H, Deguchi K, et al. MOZ-TIF2, but not BCR-ABL, confers properties of leukemic stem cells to committed murine hematopoietic progenitors. *Cancer Cell.* 2004;6(6):587-596.
27. Lozzio CB, Lozzio BB. Human chronic myelogenous leukemia cell-line with positive Philadelphia chromosome. *Blood.* 1975;45(3):321-334.
28. Okuno Y, Suzuki A, Ichiba S, et al. Establishment of an erythroid cell line (JK-1) that spontaneously differentiates to red cells. *Cancer.* 1990;66(7): 1544-1551.
29. Kubonishi I, Miyoshi I. Establishment of a Ph1 chromosome-positive cell line from chronic myelogenous leukemia in blast crisis. *Int J Cell Cloning.* 1983;1(2):105-117.
30. Gotoh A, Miyazawa K, Ohyashiki K, et al. Tyrosine phosphorylation and activation of focal adhesion kinase (p125FAK) by BCR-ABL oncoprotein. *Exp Hematol.* 1995;23(11):1153-1159.
31. Di Noto R, Luciano L, Lo Pardo C, et al. JURL-MK1 (c-kit(high)/CD30-/CD40-) and JURL-MK2 (c-kit(low)/CD30+/CD40+) cell lines: 'two-sided' model for investigating leukemic megakaryocytopoiesis. *Leukemia.* 1997;11(9):1554-1564.
32. Lee SY, Kumano K, Masuda S, et al. Mutations of the Notch1 gene in T-cell acute lymphoblastic leukemia: analysis in adults and children. *Leukemia.* 2005;19(10):1841-1843.
33. Allenspach EJ, Maillard I, Aster JC, Pear WS. Notch signaling in cancer. *Cancer Biol Ther.* 2002;1(5):466-476.
34. Fu L, Kogoshi H, Nara N, Tohda S. NOTCH1 mutations are rare in acute myeloid leukemia. *Leuk Lymphoma.* 2006;47(11):2400-2403.
35. Ingram WJ, McCue KI, Tran TH, Hallahan AR, Wainwright BJ. Sonic Hedgehog regulates Hes1 through a novel mechanism that is independent of canonical Notch pathway signalling. *Oncogene.* 2008;27(10):1489-1500.
36. Kamakura S, Oishi K, Yoshimatsu T, Nakafuku M, Masuyama N, Gotoh Y. Hes binding to STAT3 mediates crosstalk between Notch and JAK-STAT signalling. *Nat Cell Biol.* 2004;6(6):547-554.
37. Nerlov C. C/EBPalpha mutations in acute myeloid leukaemias. *Nat Rev Cancer.* 2004;4(5):394-400.
38. Gombart AF, Hofmann WK, Kawano S, et al. Mutations in the gene encoding the transcription factor CCAAT/enhancer binding protein alpha in myelodysplastic syndromes and acute myeloid leukemias. *Blood.* 2002;99(4):1332-1340.
39. Smith ML, Cavenagh JD, Lister TA, Fitzgibbon J. Mutation of CEBPA in familial acute myeloid leukemia. *N Engl J Med.* 2004;351(23):2403-2407.
40. Zhang P, Iwasaki-Arai J, Iwasaki H, et al. Enhancement of hematopoietic stem cell repopulating capacity and self-renewal in the absence of the transcription factor C/EBP alpha. *Immunity.* 2004;21(6):853-863.
41. Koschmieder S, Halmos B, Levantini E, Tenen DG. Dysregulation of the C/EBPalpha differentiation pathway in human cancer. *J Clin Oncol.* 2009;27(4):619-628.
42. Kirstetter P, Schuster MB, Bereshchenko O, et al. Modeling of C/EBPalpha mutant acute myeloid leukemia reveals a common expression signature of committed myeloid leukemia-initiating cells. *Cancer Cell.* 2008;13(4):299-310.
43. Fan X, Mikolaenko I, Elhassan I, et al. Notch1 and notch2 have opposite effects on embryonal brain tumor growth. *Cancer Res.* 2004;64(21): 7787-7793.
44. Hallahan AR, Pritchard JI, Hansen S, et al. The SmoA1 mouse model reveals that notch signaling is critical for the growth and survival of sonic hedgehog-induced medulloblastomas. *Cancer Res.* 2004;64(21):7794-7800.
45. Jaiswal S, Traver D, Miyamoto T, Akashi K, Lagasse E, Weissman IL. Expression of BCR/ABL and BCL-2 in myeloid progenitors leads to myeloid leukemias. *Proc Natl Acad Sci U S A.* 2003;100(17):10002-10007.
46. Cozzio A, Passegue E, Ayton PM, Karsunky H, Cleary ML, Weissman IL. Similar MLL-associated leukemias arising from self-renewing stem cells and short-lived myeloid progenitors. *Genes Dev.* 2003;17(24):3029-3035.
47. Krivtsov AV, Twomey D, Feng Z, et al. Transformation from committed progenitor to leukaemia stem cell initiated by MLL-AF9. *Nature.* 2006;442(7104): 818-822.